Ion upflow enhanced by drifting *F*-region plasma structure along the nightside polar cap boundary

J. Semeter, C. J. Heinselman, J. P. Thayer, and R. A. Doe
SRI International, Menlo Park, California, USA

H. U. Frey
Space Sciences Laboratory, University of California, Berkeley, California, USA

Received 14 May 2003; revised 8 September 2003; accepted 26 September 2003; published 19 November 2003.

[1] Conjugate observations by the incoherent scatter radar at Sondrestrom, Greenland, and the Wideband Imaging Camera (WIC) on the IMAGE satellite have been used to establish a causal relationship between drifting *F*-region plasma structure in the polar ionosphere and upward ion number flux near the poleward edge of the auroral oval. A longitudinally extended patch of enhanced *F*-region density was observed as it advected equatorward across the open-closed field line boundary and into a region of discrete auroral rays and strong ion upflow (V_i > 800 m/s at 900 km altitude). Upward velocities within the upflow region remained constant during the patch transit, such that the upflowing number flux was directly controlled by *F*-region density (both increased by a factor of 2 within the patch). Because polar cap patches and ion upflows are both longitudinally extended, quasi-stable features of the nightside polar cap boundary, the observed interaction can produce a global-scale increase in plasma density at higher altitudes where suprathermal outflows are initiated. *INDEX TERMS:* 2431 Ionosphere: Ionosphere/magnetosphere interactions (2736); 2463 Ionosphere: Plasma convection; 2407 Ionosphere: Auroral ionosphere (2704); 2475 Ionosphere: Polar cap ionosphere. **Citation:** Semeter, J., C. J. Heinselman, J. P. Thayer, R. A. Doe, and H. U. Frey, Ion upflow enhanced by drifting *F*-region plasma structure along the nightside polar cap boundary, *Geophys. Res. Lett.*, *30*(22), 2139, doi:10.1029/2003GL017747, 2003.

1. Introduction

[2] The ionosphere is the dominant source of heavy ions in the Earth's magnetosphere [*Chappell et al.*, 1987]. The transport of ions from the polar ionosphere to the plasma sheet requires a coupling between two observationally defined processes: "ion upflow," referring to the bulk upward motion of ionospheric plasma at thermal velocities <1500 m/s, and "ion outflow," referring to ions which have achieved escape velocity (~10 km/s) [*Yau and André*, 1997]. Presumably independent of ion upflow/outflow mechanisms is the horizontal transport of *F*-region plasma in the polar ionosphere. Large-scale "patches" of enhanced *F*-region density regularly enter the polar cap from the dayside where they advect antisunward in the ionospheric convection pattern [*Buchau et al.*, 1983; *Anderson et al.*, 1988]. Because of the long ion lifetime (a few hours above 300 km), plasma patches survive transport into the nightside ionosphere, where they become longitudinally deformed by the Harang discontinuity and may also be transported across the open-closed field line boundary and into the auroral zone by a small, but significant, equatorward velocity component associated with magnetic reconnection [*Robinson et al.*, 1985; *Crowley et al.*, 2000].

[3] This letter describes the interaction between an *F*-region plasma patch and a region of strong ion upflow at the poleward edge of the nightside auroral oval. A combination of elevation scans and fixed position measurements by the Sondrestrom incoherent scatter radar (ISR) were used to resolve plasma parameters (N_e, T_e, T_i, and V_i) in the vicinity of a patch as it advected into a region of strong rotational shear and upflowing ions at the polar cap boundary. The upward ion velocity within the upflow region appeared unaffected by the patch, such that upward ion number flux was directly controlled by horizontal variability in the *F*-region density. Because plasma patches and ion upflows are both longitudinally extended features of the nightside polar cap boundary, this interaction could produce a global-scale increase in plasma density at altitudes >2000 km, where suprathermal ion outflows are initiated.

2. Observations

[4] Figure 1 shows images of the far ultraviolet (FUV) auroral oval acquired by the Wide-angle Imaging Camera (WIC) on the IMAGE satellite [*Mende et al.*, 2002] during a 10-minute period on 11 February 2002. The double oval pattern in the premidnight sector first appeared as an identifiable feature at 2300 UT, after which the poleward branch faded gradually to below the detection threshold at 0030 UT. The Sondrestrom facility, indicated by the white circle at 74° MLAT in Figure 1, was located within a few degrees of the poleward auroral boundary during this entire period. As we shall see, the fortuitous location of Sondrestrom and the consistency of the magnetospheric configuration mitigated the usual spatial-temporal ambiguities of the ISR measurements.

[5] For this experiment, the ISR was operated in a mode that interleaved fixed position measurements in the magnetic zenith (dwells) with composite elevation-azimuth scans (comp-scans). A comp-scan consists of a pair of meridional scans in planes tilted ±25° from the magnetic meridian, whereby pairs of data at a constant altitude (~400 km in this case) and MLAT are combined to form meridional maps of horizontal ion drift. The analysis

0094-8276/03/2003GL017747$05.00

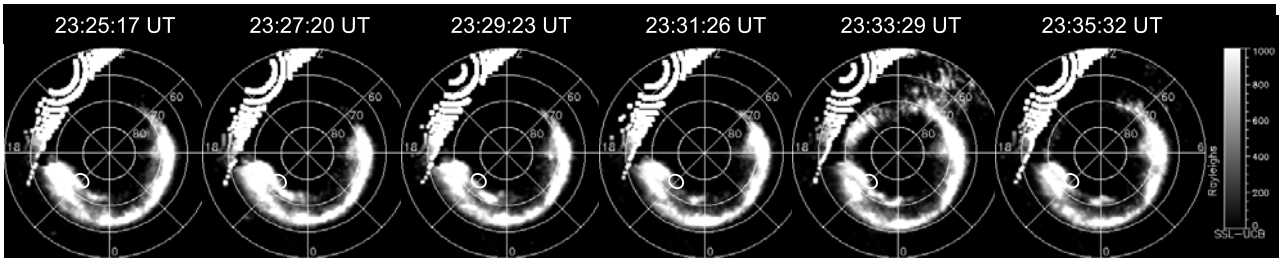

Figure 1. The FUV auroral oval observed by the IMAGE satellite during a 10 m period on 11 February 2002(in MLT–MLAT coordinates). Sondrestrom is at the center of the inset circle at 74° MLAT.

assumes longitudinal homogeneity of ~15 min MLT and temporal stability of 3.5 min, assumptions, that were quite reasonable for the dynamic time scales of interest here. The analysis also assumes $V_{\|} = 0$ at 400 km. The derived horizontal velocity will be most sensitive to this assumption near the magnetic zenith. However, as we shall see, even in regions of largest topside upflow, $V_{\|}$ at 400 km remains <100 m/s. By contrast, $V_{\perp}$ is typically >1 km/s so the maximum possible error is ~10%.

[6] Figure 2 shows horizontal ion velocity vectors for a one-hour period during which the polar cap boundary was within the field of view of Sondrestrom. The underlying color contours give the electron density at 150 km (Figure 2a) and 350 km (Figure 2b). The gaps correspond to dwell intervals. Ionization at <150 km is caused by precipitating electrons with parallel energy >1 keV. These electrons are of plasma sheet origin, that is, their flux tubes constituting closed field lines. The blue curve plots the poleward boundary of the FUV auroral oval derived independently from the space-borne image sequence. The agreement with the electron precipitation boundary is very good; the discrepancy is well within the ±150 km uncertainty in image registration. We conclude that the open-closed field line boundary lies near the poleward edge of the 150 km density enhancement in Figure 2a.

[7] The flow field in Figure 2shows a consistent latitudinal pattern with respect to this boundary. At high latitudes—within the polar cap—the flow is mostly equatorward (antisunward). Near the precipitation boundary the flow rotates eastward, signifying the presence of an equatorward electric field. Within the auroral oval the flow rotates from eastward to westward, suggesting that the large-scale meridional electric field is convergent. These features have been documented in prior Sondrestrom experiments [*Gallagher and Carovillano*, 1993; *Weber et al.*, 1991]. *Yamamoto et al.* [1993] showed that these features are also mirrored in the magnetospheric circulation; the reader is referred to this work for a discussion of electrodynamic implications. Here we are primarily concerned with the effects of *F*-region structure drifting in this flow field.

[8] Figure 2b shows that a patch of enhanced *F*-region density lies poleward of the polar cap boundary and near the eastward drift rotation. The consistent location of the

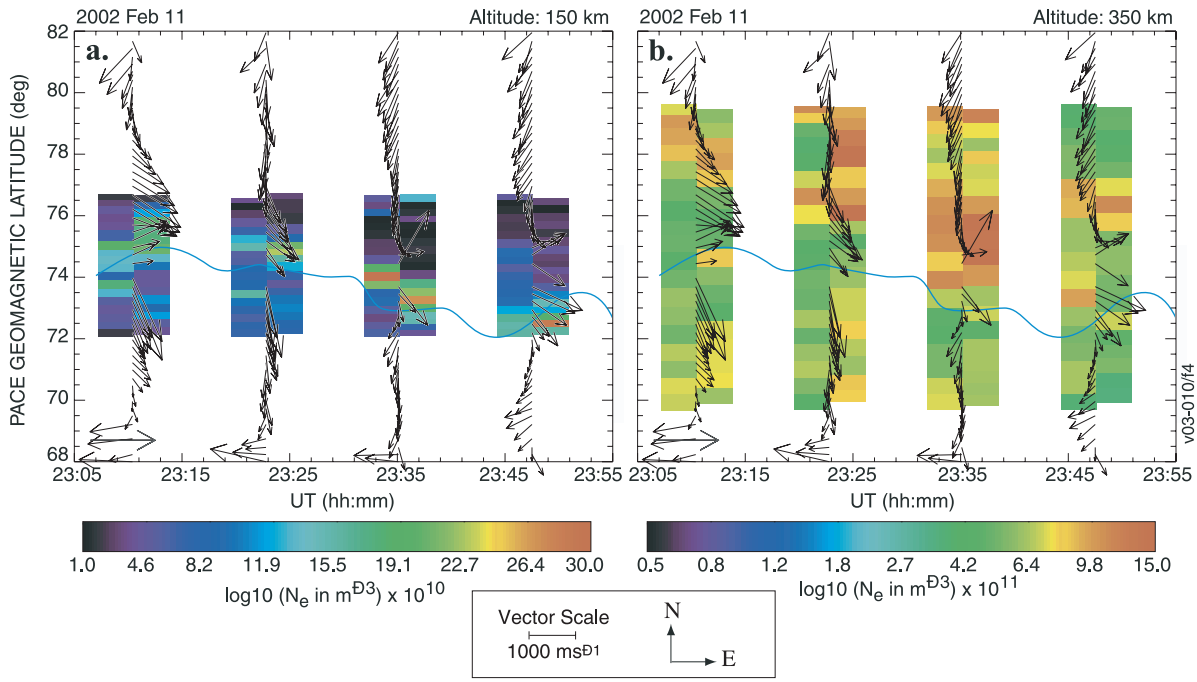

Figure 2. Vectors of horizontal ion drift superimposed on contours of electron density at (a) 150 km and (b) 350 km. The blue curve shows the location of the poleward auroral boundary derived from the satellite images.

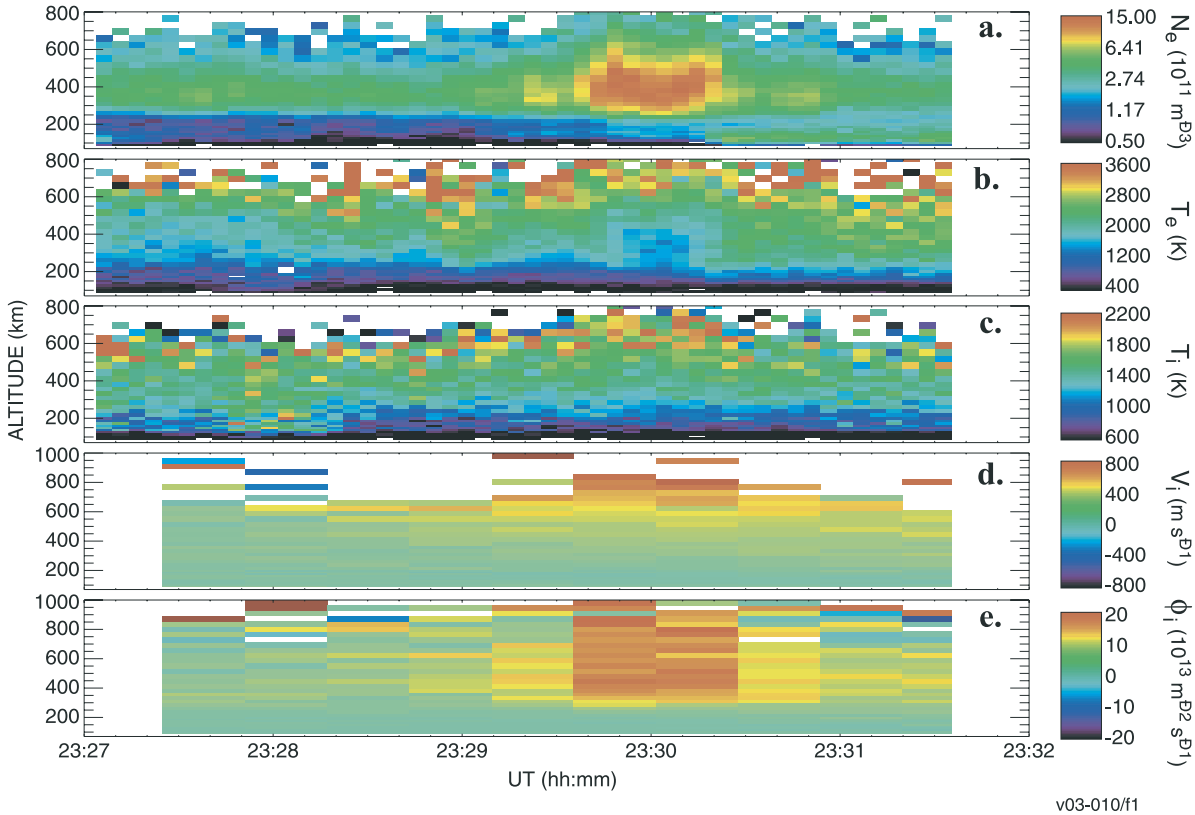

Figure 3. Sondrestrom ISR measurements of (a) electron density, (b) electron temperature, (c) ion temperature, (d) bulk upward ion velocity, and (e) bulk upward ion number flux in the magnetic zenith during transit of the polar cap boundary and *F*-region blob through the zenith. The time interval corresponds to Figure 1. Density and temperatures were processed at 5 s, while velocity and flux were processed at 30 s to achieve greater SNR on the topside.

density increase with respect to this boundary is suggestive of a coherent *F*-region structure with longitudinal extent of at least 1 h MLT. A further examination of Figure 2 shows that the distance between the patch and the polar cap boundary decreases in the first three scans. By 23:35 UT a portion of the patch appears to overlap the auroral *E*-region. This would imply an equatorward component to the ion drift directed across the open-closed field line boundary—a signature of reconnection [*de la Beaujardiere et al.*, 1991]. The transport of polar cap patches into the auroral zone under the action of reconnection has been previously investigated [*Robinson et al.*, 1985]. We now demonstrate the implications of this process for nightside ion upflow.

[9] Figure 3 shows profiles of plasma parameters in the 23:27 to 23:32 UT interval, when the patch transited the Sondrestrom zenith. The patch appears as a transient increase in N_e above 200 km from 23:29:40 to 23:30:20 UT. Note that the increased N_e alters neither the peak altitude nor the scale height of the *F*-region, and is strictly anticorrelated with T_e. These features identify the source of the N_e increase as drifting structure in the ambient plasma, and not local ionization by soft precipitation.

[10] Evidence for energetic electron precipitation can be seen throughout Figure 3a as a sporadic layer below 200 km. It is likely that Sondrestrom is within the auroral zone during the entire dwell period. The largest auroral *E*-layer occurs just after the passage of the patch, but there is clearly precipitation within the patch interval as well. This confirms the prior assertion that at least part of the patch has penetrated the open-closed field line boundary by this time.

[11] From Figure 3d we see that bulk upward ion velocities exceeded 200 m/s at 600 km throughout most of this dwell. In the 2327:30 to 2331:30 UT interval an increase in backscatter power was afforded by the patch, allowing V_i to be resolved up to 900 km where upward velocities exceeded 1 km/s. We note that during dwell periods with no aurora near the zenith, upward velocities were essentially 0. We thus observe a clear correlation between ion upflow and auroral precipitation—similar to upflows studied in the main auroral oval by *Jones et al.* [1988] and *Wahlund et al.* [1992]—however, there is no obvious causative relationship with T_e or T_i. Thus, thermal expansion cannot be the primary mechanism producing polar cap boundary upflows.

[12] Finally, Figure 3e shows that upward ion number flux increased at all altitudes above 200 km within the patch interval.

[13] To better quantify these observations, Figure 4 shows one-minute averages of N_e, V_i, and ϕ_i for three intervals: (1) 23:28:30–23:29:30 (before the patch), (2) 23:29:30–23:30:30 (during the patch), and (3) 23:31:30–23:32:30 (after the patch). The auroral *E*-region can be seen to increase in each interval. The V_i profile, on the other hand, varied very little. Thus upflow velocity is not correlated with auroral energy flux for this event. Next, note that N_e and ϕ_i both increased by a factor of ~2 above

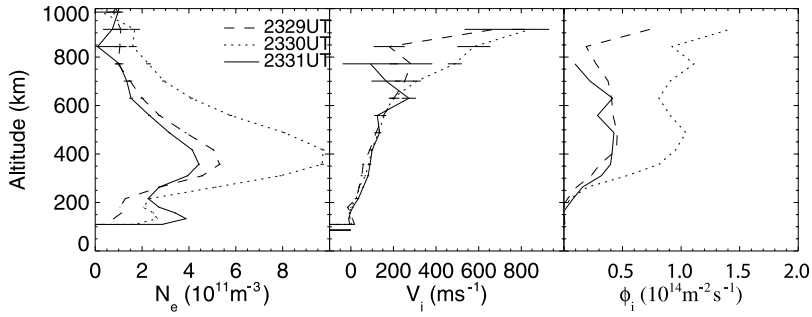

Figure 4. N_e, V_i, and ϕ_i at one-minute resolution for three intervals: before (dashed), during (dotted), and after (solid) transit of the *F*-region patch.

200 km during interval (2). The constancy in upflow velocity means that upward ion flux was directly controlled by *F*-region density for this event.

3. Discussion and Summary

[14] The observations described herein suggest a connection between horizontal plasma transport on the dayside and vertical plasma transport along the nightside polar cap boundary, i.e.:

[15] (1) Large-scale patches of *F*-region plasma enter the polar cap near local noon [*Foster and Doupnik*, 1984] and drift antisunward where they become longitudinally deformed by the Harang discontinuity. The longitudinal deformation continues in the sunward return flow along the polar cap boundary [*Robinson et al.*, 1985; *Crowley et al.*, 2000].

[16] (2) Although the flows that deform patches are largely zonal, there is a small equatorward component associated with magnetic reconnection [*de la Beaujardiere et al.*, 1991]. The action of reconnection transports patches onto closed field lines which, in turn, increases the reservoir of ions available for magnetospheric extraction.

[17] (3) Recently reconnected field lines threading the polar cap boundary support large ion upflows. Upward velocities in this region are unaffected by the introduction of patches, leading to a direct proportionality between *F*-region density and upward number flux.

[18] The consistent latitudinal pattern in Figure 2 suggests that plasma patches can have a long residency time within upflow regions. It is of interest to consider the effect of this stable interaction region on *F*-region density. Referring to Figure 4, we see that ϕ_i is strongly divergent below 400 km, increasing from 0 at 200 km to 10^{14} $m^{-2}s^{-1}$ at 400 km. Assuming vertical transport is the dominant loss mechanism in the upflow channel, the measured plasma density of 10^{11} m^{-3} at 400 km would be evacuated in 3 to 4 m. In steady state, we should expect a depletion in the bottomside of the *F*-region. Evidence for this can be seen in Figure 3a by comparing densities in the 300 to 400 km range before and after ~23:30 UT. This effect probably also contributed to the large reduction in the 350 km density at 23:47 UT in Figure 2b.

[19] The broad longitudinal extent of both the patch and the upflow means that their interaction could have a global-scale effect on the transport of ionospheric ions to the magnetosphere. As stated in the introduction, auroral ion outflow is a two-step process. To affect outflowing number flux the underlying ionospheric process need only increase upward number flux to ~2000 km altitude, where suprathermal energization is initiated [*Giles et al.*, 1994]. For the topside velocities of 1 km/s observed here, 2000 km would be reached in ~30 min, which is less than the residency time of the patch within the upflow channel in Figure 2. If all of the upflowing ions reach the energization region—either in their initial form (mostly O^+), or as lighter ions (H^+ or H_e^+) via charge exchange—then the factor-2 increase in upward flux in Figure 4 will produce a factor-2 increase in outward flux to the plasma sheet.

[20] In closing, we note that the cause of the large upward ion velocities described herein remains to be determined. Although enhancements in T_e and T_i often accompany arc-related ion upflows in the main oval [*Jones et al.*, 1988; *Wahlund et al.*, 1992], plasma temperatures remained within normal quiescent ranges for this event. In fact, Figure 3 shows that T_e decreased during the patch interval when topside velocities exceeding 800 m/s were observed. There is thus no compelling evidence for soft precipitation [*Su et al.*, 1999] or magnetospheric heat flux [*Caton et al.*, 1996] as a driver for these upflows.

References

Anderson, D. N., J. Buchau, and R. A. Heelis, Origin of density enhancements in the winter polar cap ionosphere, *Rad. Sci.*, *23*, 513–519, 1988.

Buchau, J., B. W. Reinisch, E. J. Weber, and J. G. Moore, Structure and dynamics of the winter polar cap *F*-region, *Rad. Sci.*, *18*, 995–1010, 1983.

Caton, R., J. L. Horwitz, P. G. Richards, and C. Liu, Modeling of F-region ionospheric upflows observed with EISCAT, *Geophys. Res. Lett.*, *23*, 1537–1540, 1996.

Chappell, C. R., T. E. Moore, and J. H. Waite Jr., The ionosphere as a fully adequate source of plasma for the Earth's magnetosphere, *J. Geophys. Res.*, *92*, 5896, 1987.

Crowley, G., A. J. Ridley, D. Deist, S. Wing, D. J. Knipp, B. A. Emery, J. Foster, M. Hairston, and B. W. Reinisch, Transformation of high-latitude ionospheric *F*-region patches into blobs during the March 21, 1990, storm, *J. Geophys. Res*, *105*, 5215–5230, 2000.

de la Beaujardiere, O., L. R. Lyons, and E. Friis-Christensen, Sondrestrom radar measurements of the reconnection electric field, *J. Geophys. Res.*, *96*, 13,907–13,912, 1991.

Foster, J. C., and J. R. Doupnik, Plasma convection in the vicinity of the dayside cleft, *J. Geophys. Res.*, *89*, 9107–9113, 1984.

Gallagher, H. A., and R. L. Carovillano, Plasma flows associated with an auroral arc at the polar cap boundary, *Auroral Plasma Dynamics, Geophysical Monograph*, *80*, 81–87, 1993.

Giles, B. L., C. R. Chappell, T. E. Moore, R. H. Comfort, and J. H. Waite Jr., Statistical survey of pitch angle distributions in core (0–50 eV) ions from Dynamics Explorer 1: Outflow in the auroral zone, polar cap, and cusp, *J. Geophys. Res.*, *99*, 17,483–17,501, 1994.

Jones, G. O. L., P. J. S. Williams, K. J. Winser, M. Lockwood, and K. Suvanto, Large plasma velocities along the magnetic field line in the auroral zone, *Nature*, *336*, 231, 1988.

Mende, S. B., H. U. Frey, C. W. Carlson, J. McFadden, J.-C. Grard, B. Hubert, S. A. Fuselier, G. R. Gladstone, and J. L. Burch, IMAGE and FAST observations of substorm recovery phase aurora, *Geophys. Res. Letter.*, *29*, doi:10.1029/2001GL013027, 2002.

Robinson, R. M., R. T. Tsunoda, J. F. Vickrey, and L. Guerin, Sources of *F*-region ionization enhancements in the nighttime auroral zone, *J. Geophys. Res.*, *90*, 7533–7546, 1985.

Su, Y.-J., R. G. Caton, J. L. Horwitz, and P. G. Richards, Systematic modeling of soft electron precipitation effects on high-latitude *F*-region and topside ionospheric upflows, *J. Geophys. Res.*, *104*, 153, 1999.

Wahlund, J.-E., H. J. Opgenoorth, I. Häggström, K. J. Winser, and G. O. L. Jones, EISCAT observations of topside ionospheric ion outflows during auroral activity: Revisited, *J. Geophys. Res.*, *97*, 3019–3037, 1992.

Weber, E. J., J. F. Vickrey, H. Gallagher, L. Weiss, C. J. Heinselman, R. A. Heelis, and M. C. Kelly, Coordinated radar and optical measurements of stable auroral arcs on the polar cap boundary, *J. Geophys. Res.*, *96*, 17,847–17,863, 1991.

Yamamoto, T., et al., Meridional structures of electric potentials relevant to premidnight discrete auroras: A case study from Akebono measurements, *J. Geophys. Res.*, *98*, 11,135–11,152, 1993.

Yau, A. W., and M. André, Sources of ion outflow in the high latitude ionosphere, *Space Sci. Rev.*, *80*, 1–25, 1997.

J. Semeter, C. J. Heinselman, J. P. Thayer, and R.A. Doe, SRI International, 333 Ravenswood Avenue, Menlo Park, CA 94025, USA. (Joshua.Semeter@sri.com)

H. U. Frey, Space Sciences Laboratory, University of California, Berkeley, Centennial Drive at Grizzly Peak Blvd., Berkeley, CA 94720-7450, USA.